

## Pressure-Induced Disordering and Anomalous Lattice Expansion in $\text{La}_2\text{Zr}_2\text{O}_7$ Pyrochlore

F. X. Zhang,<sup>1</sup> M. Lang,<sup>1</sup> Zhenxian Liu,<sup>2</sup> and R. C. Ewing<sup>1,\*</sup>

<sup>1</sup>*Department of Geological Sciences, University of Michigan, Ann Arbor, Michigan 48109, USA*

<sup>2</sup>*Geophysical Laboratory, Carnegie Institution of Washington, Washington, D.C. 20015, USA*

(Received 2 February 2010; published 30 June 2010)

Pressure-induced cation and anion disordering in  $\text{La}_2\text{Zr}_2\text{O}_7$  pyrochlore is quantitatively analyzed by Rietveld refinement of *in situ* x-ray diffraction patterns, Raman, and infrared measurements. An anomalous lattice expansion and obvious change of the pressure dependence of the vibrational modes occur at  $\sim 10$  GPa. The pressure-induced water incorporation in the  $\text{La}_2\text{Zr}_2\text{O}_7$  pyrochlore structure may be related to a previously noted photoelectrochemical effect.

DOI: 10.1103/PhysRevLett.105.015503

PACS numbers: 62.50.-p, 61.43.-j, 81.40.Vw

Pyrochlore oxides with the general formula  $A_2B_2X_6Y$ , where  $A$ ,  $B$  are cations and  $X$ ,  $Y$  are anions, are very important ceramics and have received considerable attention because of their many technological applications [1–3]. The structure of pyrochlore can accommodate a diverse chemistry, including over 500 synthetic compositions. The  $A$ -site ( $16d$ ) coordination polyhedron is a distorted cube that generally contains larger cations; the  $B$  site ( $16c$ ) is a distorted octahedron; the  $Y$  anion site ( $8b$ ) may be empty. Under certain conditions, such as ion irradiation, the cations are disordered over the  $A$  and  $B$  sites, and the  $X$  ( $48f$ ) and  $Y$  anion sites can be occupied by both anions and vacancies, resulting in an order-disorder transition from pyrochlore to defect-fluorite structure [2–4]. The simultaneous disordering of both cations and anions in pyrochlore is quite unique, leading to important applications.

Experimental and theoretical investigations [5–10] have shown that some pyrochlore oxides, such as  $\text{Gd}_2\text{Zr}_2\text{O}_7$  are highly radiation resistant making them an important nuclear material [8–10]. Doping with specific cations changes their transport properties and makes some compositions good ionic conductors [11,12].

$\text{La}_2\text{Zr}_2\text{O}_7$  is an ordered pyrochlore structure at ambient conditions. Upon ion irradiation,  $\text{La}_2\text{Zr}_2\text{O}_7$  easily changes to a disordered fluorite structure [13] because of the low formation energy ( $\sim 2$  eV) of the cation antisite defects [14,15]. The ease of formation of defect fluorite suggests that  $\text{La}_2\text{Zr}_2\text{O}_7$  should have a high radiation resistance. However,  $\text{La}_2\text{Zr}_2\text{O}_7$  is the only lanthanide zirconate pyrochlore that is easily amorphized upon high dose ion irradiation, though the critical temperature is quite low (310 K) [13].  $\text{La}_2\text{Zr}_2\text{O}_7$  is also very reactive with water, and it is a prominent photoelectrochemical catalyst [16,17], which can split a water molecule, yielding free protons. Proper doping of the cation site in  $\text{La}_2\text{Zr}_2\text{O}_7$  leads to the formation of a good proton conductor, suitable for electrode materials in high-temperature fuel cells [16–18]. Previously, we have found that pressure can induce structural changes and disordering of cations and anions in pyrochlore oxides [19–22], and the formation energy of defects plays a key role in controlling the extent of disorder

in the structure [22]. Structural disordering in pyrochlore is closely related to its composition and external parameters, such as energy deposition by ion irradiation, temperature, and pressure. Up to now, the formation of defects in pyrochlore oxides has been well studied theoretically [8,10,22]; however, the quantitative determination of cation and anion disordering as a function of the external conditions has not been thoroughly explored. In this Letter, we present synchrotron x-ray diffraction (XRD) results of  $\text{La}_2\text{Zr}_2\text{O}_7$  pyrochlore together with Raman scattering and infrared measurements at high pressures that provide the basis for the quantitative analysis of cation disordering and anion migration. In addition, we have discovered an anomalous volume expansion in  $\text{La}_2\text{Zr}_2\text{O}_7$  at  $\sim 10$  GPa due to the interaction of water with the pyrochlore structure, which may be related to a photoelectrochemical effect during photon irradiation.

High-pressure experiments were performed with symmetric diamond anvil cells (DAC) at room temperature by using  $\text{La}_2\text{Zr}_2\text{O}_7$  powder sample and stainless steel gasket. For the XRD measurements, different pressure media, such as Ar, methanol/ethanol mixture with or without water were used. The *in situ* XRD patterns and infrared spectra were collected at X17C and U2A stations of National Synchrotron Light Source, respectively. A monochromatic x-ray beam with energy of 30.5 keV was used for XRD measurements. The diffraction patterns were integrated from the collected images with a CCD detector using the program FIT2D [23]. The unit cell parameters were derived from the refinement of the patterns using the Rietveld method with the program FullProf [24]. Pressures in all the experiments were measured by the ruby fluorescence method [25]. Raman scattering was measured with a liquid nitrogen cooled CCD detector with an argon laser (514.53 nm) as an activation source. The IR data were collected in the far-IR (FIR) region ( $< 700$   $\text{cm}^{-1}$ ) with a helium-cooled Ge detector.

Cation antisite defects are intrinsic in rare earth zirconate pyrochlores, and the cation disorder in pyrochlore can be quantitatively analyzed through Rietveld refinement of the XRD patterns due to the large difference between the

x-ray scattering coefficients of the cations on the *A* and *B* sites. For  $\text{Gd}_2\text{Zr}_2\text{O}_7$ , the XRD refinement revealed that it can reach  $\sim 40\%$  mixed cations for the high-temperature synthetic samples. La is the largest ion among all the rare earth elements, and  $\text{La}_2\text{Zr}_2\text{O}_7$  thus has the least structural disordering. Rietveld refinement of the XRD pattern of  $\text{La}_2\text{Zr}_2\text{O}_7$  at ambient conditions revealed that the starting material has less than 20% cation disordering. In addition to cation disorder, the disordering of anion vacancies in pyrochlore also affects the XRD pattern. The only variable atomic coordinate,  $x_{48f}$ , in the pyrochlore structure can be used to quantify anion disorder. The ideal value of  $x$  in a completely disordered fluorite structure is 0.375. At high pressure, the disordering of cations and anions are two competitive factors, which influence the XRD patterns. However, simulation of XRD patterns shows that they have different effects on the relative intensity of individual peaks. Disordering of cations over the two sites makes the pyrochlore structure more like a defect fluorite structure, and as a result, all of the diffraction peaks with odd Miller indices (from the superlattice) have reduced intensities. For anions, variation of  $x_{48f}$  has different influences on individual diffraction peaks, for which the intensity can increase, decrease or show no change. The influence of cation and anion disordering on some diffraction maxima is completely different, as an example the increase of cation disorder decreases the intensity of peak (111), while anion disordering leads to an increase in its intensity. Thus, Rietveld refinement of XRD patterns at high pressure can be used to infer the degree of disorder for both cations and anions.

Selected XRD patterns of  $\text{La}_2\text{Zr}_2\text{O}_7$  at various pressures are shown in Fig. 1. At pressures higher than 21 GPa,

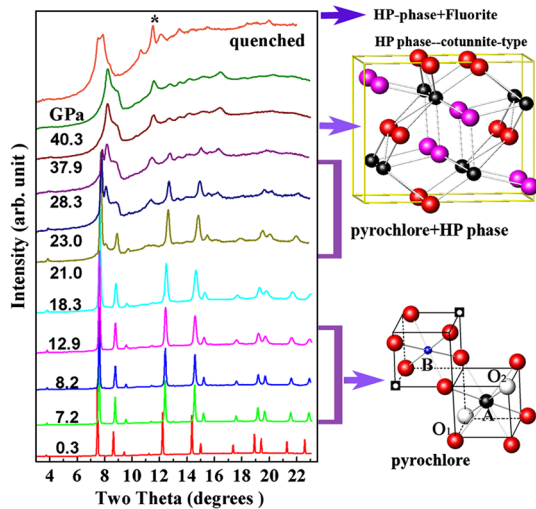


FIG. 1 (color online). Selected XRD patterns of  $\text{La}_2\text{Zr}_2\text{O}_7$  at different pressures. Below 21 GPa, the structure is pyrochlore. A distorted cotunnite-type high-pressure structure starts to form after 21 GPa and the phase transition is complete after 37.9 GPa. The quenched sample is a mixture of the high-pressure phase and defect fluorite (peak marked with a star is from the gasket).

$\text{La}_2\text{Zr}_2\text{O}_7$  starts to transform to a high-pressure phase, which is isostructural with the high-pressure phase of  $\text{Gd}_2\text{Zr}_2\text{O}_7$  [20]. The high-pressure phase is a distorted cotunnite-type structure [19] with orthorhombic or even lower symmetry, and both cations and anion vacancies are fully disordered. The high-pressure phase is not quenchable, and it changes gradually to a disordered fluorite structure during release of pressure. However, the pressure-induced atomic disordering in pyrochlore zirconate is irreversible because both the defect-fluorite and the high-pressure phase are disordered.

Cation disorder can be quantified with the cation order parameter  $\Phi_c$ . Assuming  $\Phi_c$  is 1 and 0 in ideal pyrochlore and ideal fluorite structures, respectively, the cation order parameter will be defined as [26]

$$\Phi_c = 2A_A - 1, \quad (1)$$

where  $A_A$  is the actual *A* ion occupation of the *A* site. The observed XRD patterns of  $\text{La}_2\text{Zr}_2\text{O}_7$  before the phase transition can be well refined with the pyrochlore structure model after accounting the cationic disordering [Fig. 2(a)]. Figure 2(c) shows the degree of cation disordering in  $\text{La}_2\text{Zr}_2\text{O}_7$  at various pressures. With an increase of pressure, the degree of cation disordering between  $\text{La}^{3+}$  and  $\text{Zr}^{4+}$  increases from 0.18 at ambient pressure to 0.55 at pressure of 23 GPa. On release of pressure at 23 GPa, the cation disordering process is partially reversible, and there are still 30 percent cations disordered in the quenched sample. When the sample is quenched from high pressures ( $>40$  GPa), the pressure-induced disordering is completely irreversible, and the quenched sample is a mixture

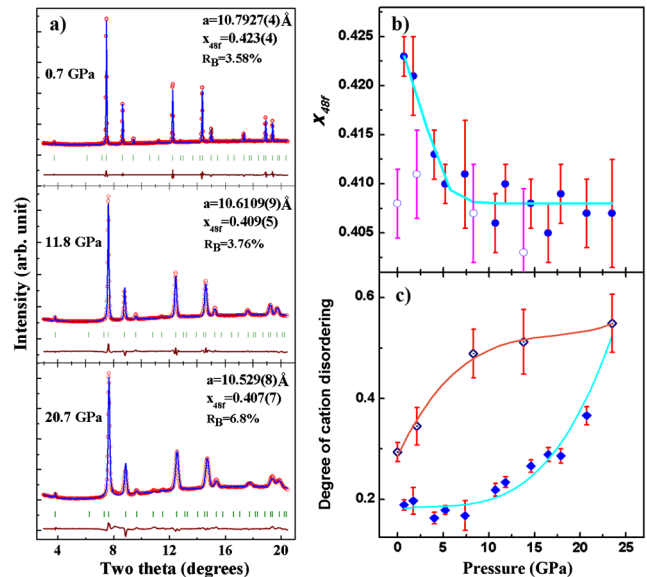


FIG. 2 (color online). (a) Refined XRD patterns of  $\text{La}_2\text{Zr}_2\text{O}_7$  at 0.7, 11.8, and 20.7 GPa, respectively; (b) Pressure dependence of  $x_{48f}$ ; (c) Degree of cation disordering with increase of pressure. The open symbols in Figs (b) and (c) were measured during release of pressure. The pressure medium is methanol-ethanol-water.

of defect-fluorite and the high-pressure phase. This is due to the energy barriers between ordered pyrochlore and the disordered states. As stated before, the only variable atomic coordinate in pyrochlore structure— $x_{48f}$  can be used as a quantitative scale of the degree of anion disordering. Figure 2(b) shows the pressure dependence of  $x_{48f}$  with pressure. Below 5 GPa,  $x_{48f}$  decreases rapidly with the increase of pressure. However, it changes very little at higher pressures. At the same time, the degree of cationic disordering does not change significantly below  $\sim 10$  GPa [Fig. 2(c)]. From this analysis, we can clearly conclude that at high pressure, the anion disordering in  $\text{La}_2\text{Zr}_2\text{O}_7$  precedes the formation of cation antisite defects. This is consistent with defect formation energy calculations in  $\text{Gd}_2\text{Zr}_2\text{O}_7$  [22] and transmission electron microscopy observations of ion irradiated rare earth zirconates [27].

The normalized profile of XRD patterns around the first diffraction maximum (111) at various pressures is shown as an insert in Fig. 3. At pressures below 10.7 GPa, the integrated intensity of the peak increased  $\sim 40\%$ , and this is caused by the anion disordering, and the value of  $x_{48f}$  decreased from 0.423 to 0.406. With increasing pressure, from 10.7 GPa to 20.7 GPa, the intensity decreased by more than 10%. This is mainly a result of cation disorder. Off course, the degree of cation disorder and the value of  $x_{48f}$  at various pressures [Figs. 2(b) and 2(c)] from the Rietveld refinement are based on the calculation of all the observed diffraction peaks.

The pressure-volume curves of  $\text{La}_2\text{Zr}_2\text{O}_7$  consistently show some slope change even with the anomalous lattice

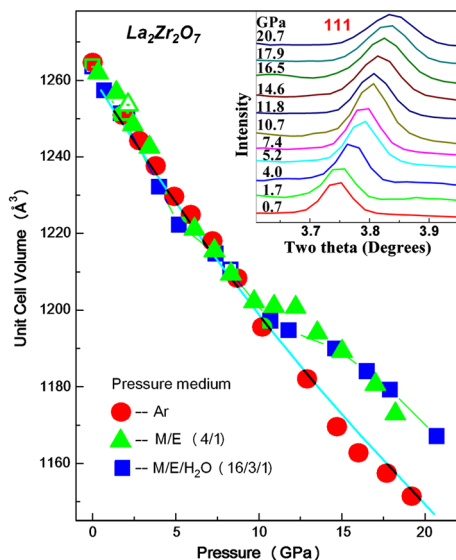


FIG. 3 (color online). Pressure ( $P$ )-volume ( $V$ ) curves for  $\text{La}_2\text{Zr}_2\text{O}_7$  pyrochlore measured with different pressure media. The  $P$ - $V$  curve of the case with Ar pressure medium can be well fit with the Brich-Murnaghan (B-M) equation of state. Open symbols were measured during release of pressure. The inset is the profile of the XRD pattern around the (111) peak (normalized) during pressurization with the M/E/ $\text{H}_2\text{O}$  pressure medium.

expansion at  $\sim 10$  GPa, when methanol/ethanol with or without water were used as pressure media (Fig. 3). The pressure experiment with Ar as the pressure medium has no such anomalous volume change, which suggests that the lattice expansion is due to the interaction of water with the pyrochlore structure. The ethanol in these experiments always contained 5% water, that is the reason why we observed the volume expansion with only methanol-ethanol as the pressure medium. This process is reversible, which suggests water intercalation into the pyrochlore structure at high pressure. Intercalation of water or other small molecules into the defect fluorite structure at the vacant  $8b$  site is not unknown [28], however, the intercalation of water into pyrochlore zirconate has not been previously reported. The documented photochemical reaction of  $\text{La}_2\text{Zr}_2\text{O}_7$  with water [16,17] may be related to the observed water intercalation at elevated pressure. The formation energy of defects in  $\text{La}_2\text{Zr}_2\text{O}_7$  is very low [14,15], small variations in external parameters, such as the pressure or irradiation with ions or even photons can create defects and make the material photochemically active. The intercalation of molecular water into  $\text{La}_2\text{Zr}_2\text{O}_7$  is probably closely related to the formation of antisite cation defects, because anion disordering mainly occurred below 5 GPa, and cation disordering occurs above  $\sim 10$  GPa. Structural disordering in pyrochlore oxides is easily realized by ion irradiation, however, there are no known results on proton conductivity or water intercalation for irradiated  $\text{La}_2\text{Zr}_2\text{O}_7$ .

Different from the heavy rare earth (such as  $\text{Gd}_2\text{Zr}_2\text{O}_7$ ) zirconate pyrochlore,  $\text{La}_2\text{Zr}_2\text{O}_7$  has quite strong and well defined Raman bands, and all five active modes are clearly observed and well separated. Atomic disorder is intrinsic in heavy rare earth zirconates, such as  $\text{Gd}_2\text{Zr}_2\text{O}_7$  where 40% of the cation sites are disordered and fully disordered in  $\text{Dy}_2\text{Zr}_2\text{O}_7$ . The strongest band at ambient conditions ( $300\text{ cm}^{-1}$ ) is complex and contains a main  $A_{1g}$  mode and a weak  $F_{2g}$  mode [Fig. 4(a)]. This band is mainly due to the vibration of oxygen in  $\text{ZrO}_6$  octahedron. We studied the intensity change of this strong mode with pressure [inset of Fig. 4(a)]. The intensity of  $A_{1g}$  mode decreases rapidly with the increase of pressure at lower pressures. This is in agreement with XRD measurements because anion defect formation precedes the formation of cation antisite defects. The Raman shift of all the modes with increasing pressure is plotted in Fig. 4(b) (normalized with values at ambient conditions), a clear slope change is observed at  $\sim 10$  GPa. This is due to the anomalous expansion of unit cell volume at this pressure, and a similar effect was also observed for the intensity of  $A_{1g}$  mode.

Water incorporation in solids can be easily detected by midinfrared techniques because of the characteristic band from OH species. However, it is very difficult to make such measurements at high pressures if water contained pressure medium is used. Generally, it is impossible to distinguish the OH species covalent bonded in the pyrochlore structure



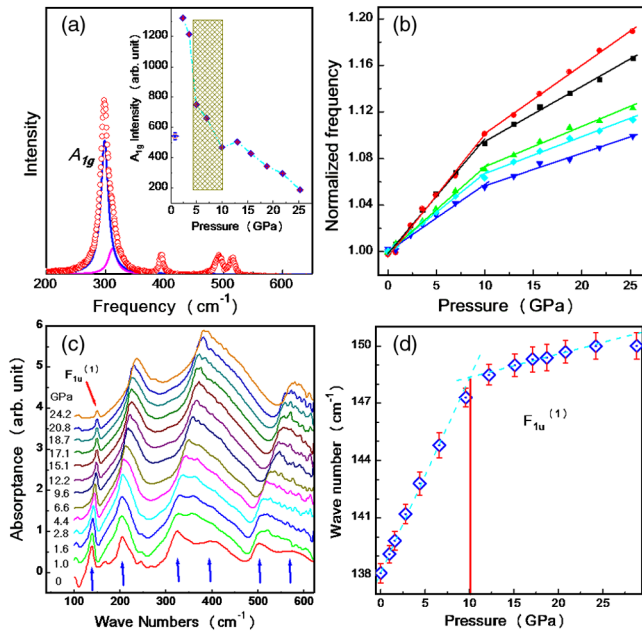


FIG. 4 (color online). (a) Typical Raman spectrum of  $\text{La}_2\text{Zr}_2\text{O}_7$  pyrochlore has five obvious modes. The inset indicates the pressure dependence of the integrated intensity of the strongest mode  $A_{1g}$ ; (b) Pressure dependence of the normalized frequencies of the five modes (Pressure media: M/E/ $\text{H}_2\text{O}$ ). (c) IR absorption spectra measured at various pressures; (d) Pressure dependence of the wave number of one sharp mode  $F_{1u}^{(1)}$  also shows a discontinuity change in the slope.

and those from free water in the pressure medium. We have successfully measured the far infrared ( $<700\text{ cm}^{-1}$ ) absorption spectrum of  $\text{La}_2\text{Zr}_2\text{O}_7$  and seven IR active modes were detected. The seventh  $T_{1g}$  mode is beyond  $600\text{ cm}^{-1}$  and is very weak. The pressure evolution of the FIR spectrum of  $\text{La}_2\text{Zr}_2\text{O}_7$  is shown in Fig. 4(c). The first  $F_{1u}$  mode is sharp and easily measured. Though it is difficult to measure the change of the intensities because of the background, the pressure dependence of the wave numbers of the first  $F_{1u}$  mode is deduced from the spectrum [Fig. 4(d)]. There is a clear change in the slope at 10 GPa. At pressures lower than 10 GPa, the frequency changes quickly with pressure and then the rate of change decreases at higher pressures. Similar to the Raman shift data, this is due to the water intercalation in the pyrochlore structure. Photochemical reaction is usually a surface-related process. In our case, water intercalation in  $\text{La}_2\text{Zr}_2\text{O}_7$  results a long-range structural change. Both the surface and interior of the samples change simultaneously, which can be detected by bulk techniques, such as XRD and IR absorption, and surface Raman scattering.

In summary, pressure-induced atomic disordering in  $\text{La}_2\text{Zr}_2\text{O}_7$  was quantitatively analyzed by XRD and a variety of spectroscopic techniques. The results clearly indicate that the formation of anion defects precede the disordering of the cations. Cation disordering occurred

mainly above 10 GPa, and this was accompanied by an anomalous lattice expansion, if water is present in the pressure medium.

This work was supported by the Office of Basic Energy Sciences of the U.S. Department of Energy, through Grant No. DE-FG02-97ER45656. The use of the x-ray beam line at X17C and infrared at the U2A station of NSLS is supported by NSF COMPRES EAR01-35554 and by US-DOE contract DE-AC02-10886.

\*Corresponding author.

rodewing@umich.edu

- [1] B. J. Wuensch and K. W. Eberman, *JOM* **52**, 19 (2000).
- [2] J. Lian *et al.*, *Acta Mater.* **51**, 1493 (2003).
- [3] N. J. Hess *et al.*, *J. Phys. Chem. B* **106**, 4663 (2002).
- [4] M. A. Subramanian, G. Aravamudan, and G. V. SubbaRao, *Prog. Solid State Chem.* **15**, 55 (1983).
- [5] S. X. Wang *et al.*, *J. Mater. Res.* **14**, 4470 (1999).
- [6] K. E. Sickafus *et al.*, *Nature Mater.* **6**, 217 (2007).
- [7] A. Meldrum, C. W. White, V. Keppens, L. A. Boatner, and R. C. Ewing, *Phys. Rev. B* **63**, 104109 (2001).
- [8] K. E. Sickafus *et al.*, *Science* **289**, 748 (2000).
- [9] R. C. Ewing, W. J. Weber, and J. Lian, *J. Appl. Phys.* **95**, 5949 (2004).
- [10] A. Chartier, G. Catillon, and J. P. Crocombette, *Phys. Rev. Lett.* **102**, 155503 (2009).
- [11] S. A. Kramer and H. L. Tuller, *Solid State Ionics* **82**, 15 (1995).
- [12] P. K. Moon and H. L. Tuller, *Solid State Ionics* **28–30**, 470 (1988).
- [13] J. Lian *et al.*, *Phys. Rev. B* **66**, 054108 (2002).
- [14] A. Chartier, C. Meis, W. J. Weber, and L. R. Corvalles, *Phys. Rev. B* **65**, 134116 (2002).
- [15] A. Chartier, C. Meis, J.-P. Crocombette, L. R. Corvalles, and W. J. Weber, *Phys. Rev. B* **67**, 174102 (2003).
- [16] M. Uno *et al.*, *J. Alloys Compd.* **420**, 291 (2006).
- [17] T. Omata and S. Otsuka-Yao-Matsuo, *J. Electrochem. Soc.* **148**, E252 (2001).
- [18] J. A. Labrincha, J. R. Frade, and F. M. B. Marques, *Solid State Ionics* **99**, 33 (1997).
- [19] F. X. Zhang *et al.*, *Appl. Phys. Lett.* **92**, 011909 (2008).
- [20] F. X. Zhang *et al.*, *Phys. Rev. B* **76**, 214104 (2007).
- [21] F. X. Zhang *et al.*, *Chem. Phys. Lett.* **441**, 216 (2007).
- [22] F. X. Zhang, J. W. Wang, J. Lian, M. K. Lang, U. Becker, and R. C. Ewing, *Phys. Rev. Lett.* **100**, 045503 (2008).
- [23] A. Hammersley, Computer program, FIT 2D (ESRF, Grenoble, 1998).
- [24] J. Rodriguez-Carvajal, *Physica (Amsterdam)* **B192**, 55 (1993).
- [25] H. K. Mao, J. Xu, and P. M. Bell, *J. Geophys. Res.* **91**, 4673 (1986).
- [26] H. L. Tuller and P. K. Moon, *Mater. Sci. Eng. B* **1**, 171 (1988).
- [27] J. Lian *et al.*, *Nucl. Instrum. Methods Phys. Res., Sect. B* **218**, 236 (2004).
- [28] C. A. Perottoni and J. A. H. da Jornada, *Phys. Rev. Lett.* **78**, 2991 (1997).